



Tunnel-Free Scheme Using a Routing Table in a PMIPv6-Based Nested NEMO Environment

Sunghong Wie¹ and Jaeshin Jang^{2*}, *Member, KIICE*

¹Division of Information Technology, The Cyber University of Korea, Seoul 110-800, Korea

²Department of Information and Communications, Inje University, Gimhae 621-749, Korea

Abstract

In this paper, we propose a novel tunnel-free scheme in a proxy mobile IPv6 (PMIPv6)-based nested network mobility environment; several mobile nodes (MNs) and mobile routers (MRs) compose a hierarchical wireless network topology. Because tunnels created by several MRs overlap and data packets travel along several local mobility anchors (LMAs), the utilization of the wireless section is reduced and the packet forwarding path of the wire-line section is not optimal. In our tunnel-free scheme, the mobile access gateway (MAG) plays an important role in both the wireless and wire-line sections. Using a local binding update, this tunnel-free scheme forwards data packets with a host-based routing table without any tunnel. Establishing a direct tunnel between the MAG and the last LMA, this scheme removes nested tunnels between intermediate LMAs and MRs, and optimizes the forwarding path to the MN in the wire-line section.

Index Terms: Network mobility, PMIPv6 (proxy mobile IPv6), Routing table, Tunnel-free scheme

I. INTRODUCTION

As new mobile devices such as cellular phones, PDAs, laptop computers, and touch screen computers become more and more popular, many people want to be able to access the internet without limitations. Rapid advances in various wireless access technologies such as wideband code division multiple access (WCDMA), mobile worldwide interoperability for microwave access (M-WiMAX), long term evolution (LTE), wireless local area networks (WLANs), and wireless sensor networks (WSNs) respond to consumers' demands for mobile and ubiquitous computing environments.

As the number of network devices supporting the IPv4 protocol has been rapidly increasing, a shortage of IPv4 addresses to assign to new devices has arisen. To address the shortage in the IP address pool, the Internet Engineering Task

Force (IETF) has proposed an IPv6 protocol with 64 bit addresses [1]. However, because mobility management is not supported in IPv6, Mobile IPv6 (MIPv6) [2] has also been standardized by the IETF. MIPv6 does not define a foreign agent (FA) and supports an optimized routing path through which a mobile node (MN) can communicate directly with a correspondent node (CN). Careful consideration has been required, however, to avoid a heavy and complicated MIPv6 protocol, which could cause several critical problems in wireless mobile devices, such as poor CPU performance, a large power consumption, and a shortened battery life. To overcome these problems in wireless environments, a network-based mobility management solution called Proxy MIPv6 (PMIPv6) [3] is standardized by the IETF Network-Based Localized Mobility Management (NETLMM) working group. In a PMIPv6 protocol, the mobility management

Received 06 November 2012, Revised 23 November 2012, Accepted 12 December 2012

*Corresponding Author Jaeshin Jang (E-mail: icjoseph@inje.ac.kr, Tel: +82-55-320-3520)

Department of Information and Communications Engineering, Inje University, 197 Inje-ro, Gimhae 621-749, Korea.

Open Access <http://dx.doi.org/10.6109/jicce.2013.11.2.082>

print ISSN: 2234-8255 online ISSN: 2234-8883

© This is an Open Access article distributed under the terms of the Creative Commons Attribution Non-Commercial License (<http://creativecommons.org/licenses/by-nc/3.0/>) which permits unrestricted non-commercial use, distribution, and reproduction in any medium, provided the original work is properly cited.

Copyright © The Korea Institute of Information and Communication Engineering

function is performed by network equipment and only the IPv6 protocol stack is implemented in mobile devices for a light protocol. The PMIPv6 protocol includes two functional network entities: a local mobility anchor (LMA) and a mobile access gateway (MAG). A MAG detects the movement of an MN and initiates the mobility-related signaling with the corresponding LMA on behalf of the MN. A MAG establishes a bidirectional tunnel with an LMA through which packets for the MN are routed. An LMA is similar to a home agent (HA) in MIPv6, and the LMA contains the location information for MNs in a binding cache. Thus, a main role of an LMA is to maintain reachability to the MN's address while the MN moves around within a PMIPv6 domain.

Currently, network mobility (NEMO) solutions are being developed by the IETF. A special mobile device called the mobile router (MR) is introduced in NEMO. The MR is located in a vehicle and provides mobile devices with a communication link to the internet. The mobility framework of the NEMO basic support protocol (BSP) [4] is Mobile IPv6. In order to support the transparent access to the internet, MIPv6 should be implemented in both MRs and MNs. In order to overcome several problems of the MIPv6 protocol, some researchers are studying PMIPv6 protocols instead of MIPv6. In this paper, we propose a novel scheme that removes excessive tunnels and increases the utilization of wireless resources in PMIPv6-based NEMO environments.

The remainder of this paper is organized as follows. In Section II, we present related works about PMIPv6-based NEMO. In Section III, we propose the novel scheme. In Section IV, we provide a performance analysis on the proposed scheme and in Section V, we show various numerical results. Finally, we conclude this paper in Section VI.

II. RELATED WORKS

A representative solution for PMIPv6-based NEMO called N-PMIPv6, is proposed in [5]. The key idea of N-PMIPv6 is to extend the PMIPv6 domain to also include mobile networks. The MR operating in the N-PMIPv6 protocol performs a similar function to the MAG in a PMIPv6 protocol. For example, consider the simple MIPv6 network shown in Fig. 1, where some MNs are attached to a specific MR, and the MR initiates a binding update to the corresponding LMA. A visiting mobile node (VMN) denotes a mobile node (MN) that is outside its home network. When MR#1 detects an attachment from the VMN, it sends a signaling message to the corresponding LMA managing the VMN's address. That is, on behalf of the VMN, MR#1 initiates MIPv6's signaling procedures and deals with related messages from the corresponding LMA.

Similarly, when MR#1 attaches to MR#2, MR#2 deals with signaling messages on behalf of MR#1. Because N-PMIPv6 is a representative solution, we will make a comparison between our scheme and the N-PMIPv6 scheme in the next section. Although N-PMIPv6 is simple and scalable, a nested NEMO environment causes an inefficiency in wireless resources and the non-optimal routing path shown in Fig. 1(a). For example, multi-tunnels cause a large overhead and data packets may travel along several LMAs, as shown in Fig. 1(b). In [6], the N-NEMO scheme is proposed. N-NEMO is based on a tunnel splitting scheme composed of two parts: the global tunnel that is established between an LMA and a MAG, and a local tunnel that is established between the MR and the MAG. This tunnel splitting scheme has greater data efficiency, using less packet overhead, and reduces the latency of the packet transmission using a more optimal route. However, it does not consider multiple LMAs, and various handover procedures are not clear. A Tunnel Compress Scheme (TCS) is proposed in [7], which compresses the multi-tunnels of a routing path into two separated tunnels; one tunnel is established from MAG to LMA and the other tunnel is established from MAG to MR. Consequently, the TCS scheme reduces the inefficiency of wireless utilization and the non-optimal routing path as in N-NEMO. However, this network mobility scenario is ambiguous, and a few simulation results are not sufficient to explain the properties of the TCS scheme. In addition, the performance of the TCS scheme is not analyzed, and there is one compressed tunnel in the wireless path. In this paper, we eliminate the wireless tunnel and describe the performance analysis.

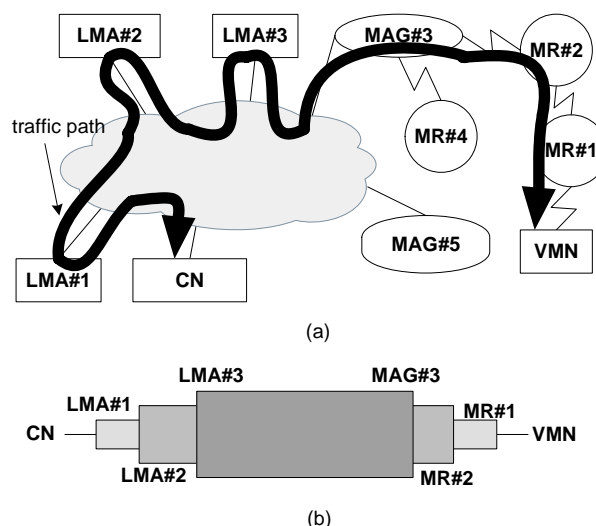


Fig. 1. Nested NEMO network topology and tunnel structure in N-PMIPv6: (a) Network topology and (b) tunnel between CN and VMN. LMA: local mobility anchor, CN: correspondent node, MAG: mobile access gateway, MR: mobile router, VMN: visiting mobile node.

Many route optimization schemes in NEMO [8] and PMIPv6 [9] are related to our interests. However, a combined study of both PMIPv6 and NEMO environments is required.

III. PROPOSED SCHEME

Fig. 1 illustrates two parts of a packet's routing path in N-PMIPv6. The first part is the wire-line section that the data packets travel through several LMAs. Because there are three nested levels and each different LMA manages the home network prefixes (HNPs) of both the MRs and VMNs, packets for the VMN travel through three LMAs. Two of the three LMAs are not essential entities and thus the wire-line part of the routing path is not optimal in Fig. 1. In order to overcome this non-optimal routing path of N-PMIPv6, our tunnel-free scheme (TFS) proposed in this paper establishes only one tunnel between the VMN's LMA and the MAG. That is, because packets for the VMN do not pass through LMA#2 and LMA#3 in the TFS scheme, the routing path of the TFS scheme is more optimal than that of the N-PMIPv6. The second part of the routing path is a wireless section consisting of one MAG, several MRs, and VMNs. The TFS scheme removes all of the tunnels in the wireless section between the MAG and the VMN. Instead of multi-tunnels, the host-based routing is performed in our TFS scheme. The multi-tunnel problem of N-PMIPv6 reduces the utilization of wireless resources and causes unnecessary packet fragmentation. In summary, the TFS scheme optimizes the route path of the wire-line section and removes all tunnels of the wireless section. Additionally, due to the route path optimization of the wire-line section, the number of related LMAs is decreased and thus the load to the LMA may be reduced.

N-PMIPv6 uses a proxy binding update (PBU) message to register a node's locations at the LMA. To support the TFS's operations, an extended PBU message is defined in Fig. 2. The TFS's PBU message of the wire-line section is the same as the N-PMIPv6's PBU message, and the extended PBU message is deployed only in the wireless section. An extended PBU message includes a T-flag that denotes the TFS's operation. Multiple TF options may be appended in an extended PBU message to register the routing table of both the MRs and a MAG. In addition, a MAG establishes a direct tunnel with an LMA, of which the information is recorded in a TF option. In order to provide full details of the TFS scheme in the network topology in Fig. 1(a), we handle several scenarios as follows.

A. VMN Joins MR#1

Fig. 1(a) shows that MR#2 is attached to MAG#3 and MR#1 is attached to MR#2. When a VMN joins MR#1, MR#1's L2 detects the new connection with the VMN and obtains an LMA address from the Authentication, Authorization and Accounting (AAA). The interaction between MR#1 and the AAA is based on the authentication protocol, but this is beyond the scope of the current study. If the N-PMIPv6 protocol is used, MR#1 generates a PBU message of which the target address is LMA#1 on behalf of the VMN. However, in the case of the TFS scheme, the target address of an extended PBU message is not LMA#1 but the next-hop address. Thus, an extended PBU message is relayed from node to node in a wireless section. The TF option for the VMN is appended to an extended PBU message by MR#1. After MR#1 saves both its TF options and a source address into an internal memory, then it forwards an extended PBU message to the next-hop entry in the direction of the MAG as shown in Fig. 3. After the MAG finally receives an extended PBU message from MR#2, it carries out a binding update by exchanging the ordinary PBU/proxy binding acknowledgement (PBA) messages with the LMA recorded in a TF option. Upon receiving a PBU message from the MAG, the LMA determines whether it accepts the request of the binding update or not. A PBA message contains a status field that represents a success or failure code in this binding update. If a success code is included in a PBA message, it triggers routing table updates of both the MAG and the MRs in the wireless section. On registering a routing entry for the VMN, both the MAG and the MRs use the internal information such as the TF option and a source address, and check other information such as the home network prefix (HNP) option in a PBA message. There are two major parts in an entry of a routing table: a destination field contained in the HNP option of a PBA message, and a next-hop field that is the source address of the PBU message.

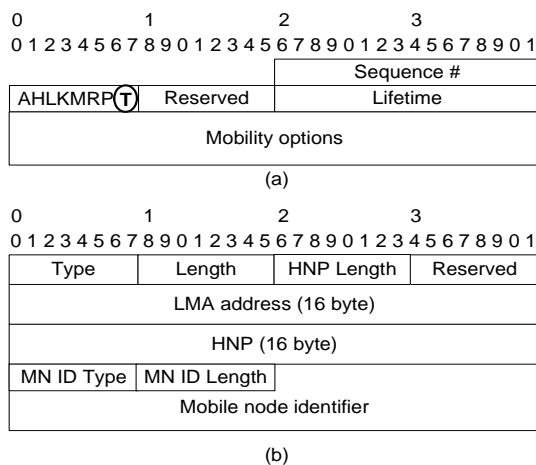


Fig. 2. (a) Extended proxy binding update message and (b) tunnel-free option. HNP: home network prefix, LMA: local mobility anchor, MN: mobile node.

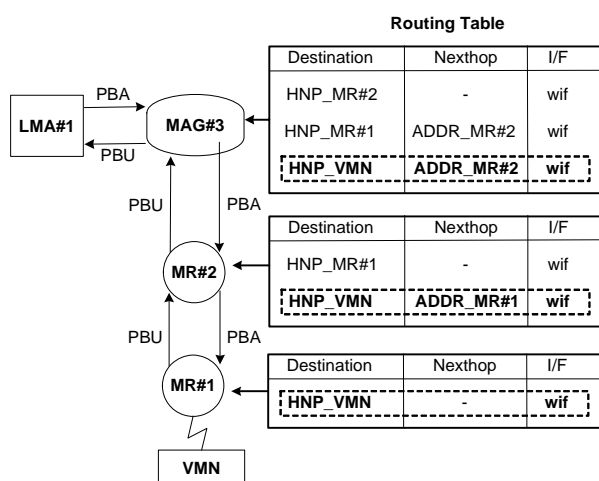


Fig. 3. Routing table update via proxy binding update/proxy binding acknowledgement (PBU/PBA) messages. LMA: local mobility anchor, MAG: mobile access gateway, MR: mobile router, HNP: home network prefix, VMN: visiting mobile node.

The TFS scheme requires a large memory for storing TF options, a source address of the PBU message, and an additional entry of the routing table.

Let's assume that an external CN sends a data packet to the VMN. In the case of N-PMIPv6, data packets from a CN to a VMN travel along LMA#1, LMA#2, and LMA#3 through nested tunnels as shown in Fig. 1. However, in our TFS scheme, the data packets are routed to LMA#1 and are encapsulated from LMA#1 to MAG#3. In MAG#3, these data packets are decapsulated and then forwarded to MR#2 by a routing table. Because the destination address of the data packets is matched with a HNP of the VMN, these data packets are forwarded to MR#2, the next-hop node. Similar operations, such as looking up a routing table, are performed in both MR#2 and MR#1. Finally, because the next-hop address field is blank in the routing entry of MR#1, the data packets are forwarded directly to the VMN.

B. Intra-MAG Handover of VMN

Although a VMN moves outside an attached MR, it may reside in the same MAG's area. This is a handover event within a MAG called the intra-MAG handover. For example, if a VMN connected to MR#1 is moving to MR#2's area in Fig. 1, then this type of movement results in an intra-MAG handover. Because the tunnel of the TFS scheme is terminated at the MAG, the topology change in a wireless section does not affect the tunnel between an LMA and a MAG. Thus, in the TFS scheme, a binding update of an intra-MAG handover is limited only to the wireless section and does not propagate into the wire-line section. Those binding update-related messages are called local PBU (LPBU) and local PBA (LPBA) messages. A signaling

procedure of an intra-MAG handover is shown in Fig. 4. As the VMN is detached from MR#1, the de-registration PBU message is initiated by MR#1. When a de-registration PBU message is relayed to MR#2, a routing entry in the MR#2 for the VMN is temporarily disabled and MR#2 triggers a temporary timer ($T_{intraMAG}$). When the timer is expired, the routing entry is removed. This temporary timer is triggered in MR#1, MR#2, and MAG#3, which receive a deregistration PBU message. On expiration of this timer, the MAG sends a de-registration PBU to the LMA. As MAG#3 receives the de-registration PBU message, it does not report this event to the LMA but responds immediately to MR#1 via MR#2 with a de-registration PBA message. Before the $T_{intraMAG}$ timer expires, the VMN is attached to MR#2, which starts a signaling procedure of a binding update. However, because MAG#3 knows that the VMN was attached to MR#1 before, it thinks this is an intra-MAG handover and does not send a PBU message to the LMA. Both MRs and the MAG stop the temporary timer ($T_{intraMAG}$) and update the routing entry for the VMN. Because an intra-MAG handover does not require interaction with the LMA, it results in low signaling overhead, a short handover latency, and a low processing load to the LMA.

C. Inter-MAG Handover of VMN

When the VMN is removed from the current MAG's area and enters the new MAG's area, the inter-MAG handover occurs. In the old MAG and the old MRs, a temporary timer, $T_{intraMAG}$, is activated, as seen in Fig. 4. As the timer expires or the binding revocation procedure from the LMA is performed, all information of the old MRs and the old MAG will be removed. In the new MAG's area, a binding update procedure is performed as shown in Fig. 3.

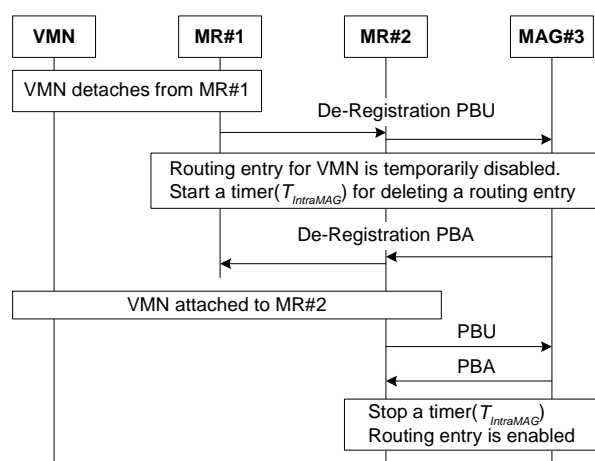
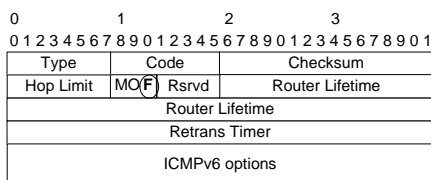


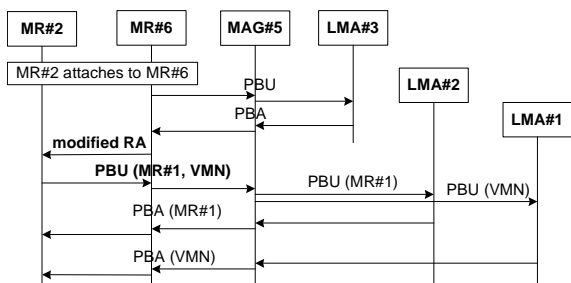
Fig. 4. Signaling procedure of Intra-MAG handover. VMN: visiting mobile node, MR: mobile router, MAG: mobile access gateway, PBU: proxy binding update, PBA: proxy binding acknowledgement.

D. Inter-MAG Handover of MR

NEMO defines a special device (e.g., MR), which can move into any place with the same IP address, even in a visiting network. Therefore, the TFS scheme needs to support the MR's mobility in various scenarios. If MR#2 detaches from MAG#3 and attaches to MR#6 of MAG#5 as in Fig. 1, an inter-MAG handover is triggered that includes both MR#1 and a VMN. MR#6 detects the attachment of MR#2 and exchanges PBU and PBA with MAG#5 and adds a routing entry for MR#2. In addition, MAG#5 establishes the tunnel with LMA#3 and adds a routing entry for MR#2. The procedures of both binding registration and the routing table update are the same as Scenario A. MR#6 can be aware of an attachment to MR#2, but cannot sense what nodes are hidden behind MR#2. To request a binding update for the hidden nodes in the TFS scheme, we define a modified router advertisement (RA) as in Fig. 5(a). In N-PMIPv6, an RA message is sent with an HNP in an option field. In the TFS scheme, a modified RA message includes two new fields: the F-flag, which is used to trigger a binding procedure for hidden nodes, and an HNP field. In this scenario, when MR#6 receives a modified RA message, it performs the binding update on behalf of two hidden nodes, MR#1 and the VMN. Because MR#2 maintains the hidden nodes' TF options and the routing entries for both MR#1 and the VMN, it already knows the binding-related information about MR#1 and the VMN. Therefore, MR#2 sends a PBU message with all of the hidden nodes' TF options as in Fig. 5(b). In that time, a PBU message operates as a group registration message for all of the hidden nodes.



(a)



(b)

Fig. 5. (a) Modified router advertisement (RA) message and (b) signaling procedure of mobile router (MR) handover. MAG: mobile access gateway, LMA: local mobility anchor, PBU: proxy binding update, PBA: proxy binding acknowledgement, VMN: visiting mobile node.

MAG#5 constructs each node's ordinary PBU message from an extended PBU message. Separately, each PBA message is responded to by each LMA and each routing entry is added in MR#6 and MAG#5. All TF options of both MR#1 and the VMN are also saved in MR#6 and MAG#5 along with the routing entries, as in scenario A.

In comparison with N-PMIPv6, the TFS scheme has some disadvantages in a MR handover scenario. It is unnecessary for hidden nodes to update their locations in N-PMIPv6. However, because the TFS scheme requires additional signaling procedures for hidden nodes, both the signaling overhead and the handover latency may increase. Nevertheless, there is room for improvement. There are two parts in the signaling procedure of Fig. 5(b). The first part is a handover procedure of representative node MR#2, and the second part is the handover procedure of hidden nodes MR#1 and the VMN after receiving a modified RA. Because it is required that these binding procedures take place in sequence, the handover latency is larger than that of N-PMIPv6. The simultaneous binding procedures may be considered a further research item. Two separate handover procedures of both the representative node and hidden nodes can proceed simultaneously after MR#2 and MR#6 detect the attachment of other nodes. This simultaneous procedure will contribute a reduction in the handover latency. However, because this is outside the scope of our current study, we describe this simultaneous binding as a possibility to improve the handover performance of the TFS scheme. Furthermore, in our TFS scheme, several binding updates from the MAG to the LMA are processed separately as shown in Fig. 5(b). If the bulk update procedure can be defined as bulk re-registration [10], the number of signaling messages can be significantly reduced.

E. Intra-MAG Handover of MR

In this intra-MAG handover, we assume that MR#2 moves to MR#4 in the same MAG#3. This scenario's signaling procedure is similar to that of scenarios B and D, but because it does not move to another MAG, the interaction between a MAG and a LMA is not required. Thus, a PBU message from MR#4 is terminated at MAG#3, and a PBA message is responded to by MAG#3. The exchanges of PBU and PBA messages are limited only in the wireless section and are used in the routing table update of immediate MRs.

F. Local Routing

A CN may be a fixed node at a wire-line section or a MN in a wireless section. Thus, if a CN is connected to the same MAG with the VMN, there is a short path between the CN and the VMN. However, data packets should always go

through a distant LMA. Because the LMA performs important functions in packet delivery, statistics gathering, accounting, and various other functions for mobile nodes, data packets should transfer through the LMA. However, the forwarding path of a data packet is not optimal and results in an unnecessary delay for packet delivery. If there are no problems in other functions such as statistics gathering and accounting, it is optimal that data packets from the VMN are directly forwarded to the CN. Thus, we call this direct forwarding policy local routing. If local routing for the VMN is enabled in either an MR or a MAG, a data packet to the VMN is not tunneled to the LMA and is directly forwarded. This local routing scheme can be feasible by defining a flag in the AAA. When a MN is attached, various policies can be obtained from the AAA. By adding a flag for the local routing policy per the MN, it is easy to control a local routing policy.

IV. PERFORMANCE ANALYSIS

In this section, we present our analysis and comparison of the performance on N-PMIPv6 and our TFS scheme. In order to compare the performance of different protocols, we use the protocol cost as the performance metric, as used in other research studies [6, 9, 11, 12]. The total cost of a MIPv6-related protocol is the sum of the cost of a binding update and a packet delivery, which is shown in Eq. (1).

$$C_T = C_{BU} + C_{PD}. \quad (1)$$

The cost of a binding update, C_{BU} , denotes the signaling cost required when a mobile node moves to another MR or MAG and sends a PBU message and receives a PBA message. The packet delivery cost, C_{PD} , denotes the traffic overhead required when data packets travel through both wire-line and wireless sections. Both a signaling cost and a packet delivery cost consist of two major parts: the product of a packet length with the hop distance, and the packet processing cost in network devices such as routers, MRs, MAGs, and LMAs.

A. System Model

In order to analyze the performance of our TFS scheme, we assume a network model as in Fig. 6. It is assumed in Fig. 6 that the nested level is M and there are multiple different LMAs managing the MRs and the VMNs. Thus, the hop distance from the MAG to the VMN is M and the number of immediate MRs located between the MAG and the VMN is $(M-1)$. We define the number of mobile nodes of level k that are connected to one MR of level $(k-1)$ as N_k .

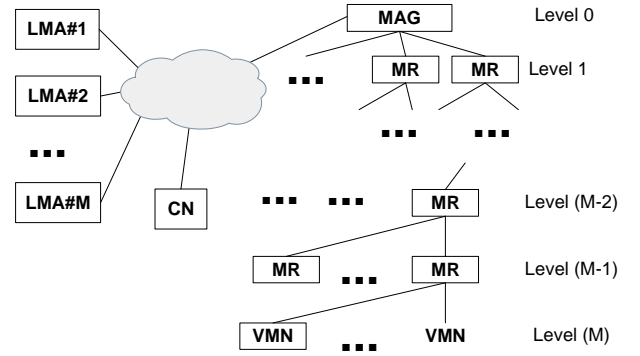


Fig. 6. Network model for performance analysis. LMA: local mobility anchor, CN: correspondent node, MAG: mobile access gateway, MR: mobile router, VMN: visiting mobile node.

There are many moving nodes such as the MRs and VMNs in Fig. 6. For simplicity, we consider one type of a mobility model per nested level and calculate the protocol cost with the assumption that a node of a specific nested level moves and all nodes of the other nested levels are fixed. We define the following new parameters as ω_k , the sum of which is 1.

ω_k = weighting factor of protocol cost that a MN of level k moves and satisfies $\sum_{k=1}^M \omega_k = 1$.

While the packet delivery cost is independent from the mobility model, the cost of the binding update is dependent on the mobility model. Thus, we can get the summation as follows:

$$C_{BU} = \sum_{k=1}^M \omega_k \cdot C_{BU}(k). \quad (2)$$

For the convenience of analyzing the performance of both N-PMIPv6 and the TFS scheme, we assume that the cell size of a MR in level k is S_k and is filled with connected cells of the MRs at level $(k+1)$. Therefore, if we assume that the smallest cell size of the MR at level $(M-1)$ is S_{M-1} , then S_k is calculated as follows:

$$S_k = S_{M-1} \cdot \prod_{j=k+1}^{M-1} N_j, \quad \text{where } (0 \leq k < M). \quad (3)$$

In the case of the MR's handover, the TFS scheme requires the binding update for hidden nodes. We therefore calculate the number of hidden terminals in view of an MR of level k as follows:

$$U_k = N_{k+1} + N_{k+1} \cdot N_{k+2} + \dots + N_{k+1} \cdot N_{k+2} \cdot \dots \cdot N_M \quad (4)$$

$$= \sum_{i=k+1}^M \left(\prod_{j=k+1}^i N_j \right).$$

We also make the following additional assumptions to derive the mobility and traffic models.

- The session arrival process follows the Poisson distribution with rate λ_s .
- There are no inter-level handovers. That is, neither MRs nor VMNs at level k move to the other MR or MAG at different levels, except level k . Although this assumption is considered unreasonable, it is not problematic when comparing protocol costs and major properties of different MIPv6-related protocols.
- The residence time during which an MR and a VMN stay in the given area follows an exponential distribution.

Let $\mu_{x,y}$ be the crossing rate by which the mobile node at level x crosses the boundary of an MR at level y . From [12], $\mu_{k,k-1}$ are expressed as follows:

$$\mu_{k,k-1} = 2v_k / \sqrt{\pi \cdot S_{k-1}}, \tag{5}$$

where $(0 < k \leq M)$ and v_k is the average velocity of the mobile node at level k . Because the MAG is located at level 0, let us define the crossing rate of the MAG's boundary as follows:

$$\begin{aligned} \mu_{k,0} &= \mu_{k,1} / \sqrt{N_1} = (\mu_{k,2} / \sqrt{N_2}) / \sqrt{N_1} \\ &= \frac{\mu_{k,k-1}}{\prod_{i=1}^{k-1} \sqrt{N_i}}, \end{aligned} \tag{6}$$

where $(0 < k \leq M)$. Using the research results in [11] with the assumption that an MR is moving at level k , we get the average number of handover events during a session interval as follows:

$$E(H_{k,k-1}) = \mu_{k,k-1} / \lambda_s. \tag{7}$$

On the same occasion, we get the average number of inter-MAG handovers during a session interval as follows:

$$\begin{aligned} E(H_{k,interMAG}) &= E(H_{k,0}) \\ &= \mu_{k,0} / \lambda_s \\ &= \frac{\mu_{k,k-1}}{\prod_{j=1}^{k-1} \sqrt{N_j} \lambda_s} \\ &= \frac{1}{SMR_k \cdot \prod_{j=1}^{k-1} \sqrt{N_j}}, \end{aligned} \tag{8}$$

where the session-to-mobility ratio (SMR) at level k is defined as $SMR_k = \lambda_s / \mu_{k,k-1}$. Because Eq. (7) contains the average number of inter-MAG handovers, we can obtain the average number of intra-MAG handovers as follows:

$$\begin{aligned} E(H_{k,intraMAG}) &= E(H_{k,k-1}) - E(H_{k,interMAG}) \\ &= (\mu_{k,k-1} - \mu_{k,0}) / \lambda_s \\ &= \frac{1}{SMR_k} \cdot \left(1 - \frac{1}{\prod_{j=1}^{k-1} \sqrt{N_j}} \right). \end{aligned} \tag{9}$$

We define here several notations for explaining our cost model in detail:

- τ : IPv6 tunneling header size, 40 bytes
- ϕ : TF option size for one mobile node, 44 bytes
- α : transmission unit cost in wired link, 1
- β : transmission unit cost in wireless link, 1.5
- L_{PBU} : PBU message size, 76 bytes
- L_{PBA} : PBA message size, 76 bytes
- L_{RA} : RA message size, 76 bytes
- PC_R : processing cost in a router, 8
- PC_{MR} : processing cost in a MR, 10
- PC_{MAG} : processing cost in a MAG, 12
- PC_{LMA} : processing cost in a LMA, 24
- $d_{VMN-MAG}$: hop distance from VMN to MAG, M hops
- $d_{MAG-LMA} = d_{LMA-MAG}$: hop distance from MAG to LMA, 20 hops
- $d_{LMA-LMA}$: hop distance from LMA to LMA, 8 hops
- d_{LMA-CN} : hop distance from LMA to CN, 10 hops

B. Performance Analysis of N-PMIPv6

Because each MR operates as a MAG in N-PMIPv6, it exchanges PBU and PBA messages with an LMA. In order to calculate the cost of a binding update with the assumption that a mobile router of level k is moving, the message type and the message traveling section should be considered. Thus, the cost for transmitting a PBU message in a wire-line section is calculated as Eqs. (10) and (11). With the weighting factor of the wireless section and the nested level of M , $C_{PBU}(k)_{wireless}$ is calculated as Eq. (12). Because a PBA message goes in the reverse direction of a PBU message, both $C_{PBA}(k)_{wireline}$ and $C_{PBA}(k)_{wireless}$ are calculated as Eq. (13). The signaling procedure is the same in either the intra-MAG or the inter-MAG handover in N-PMIPv6. Therefore, the cost of a binding update is

$$\begin{aligned}
 C_{PBU}(k)|_{\text{wireline}} &= \alpha \cdot x(L_{PBU} + \tau(k-1)) \\
 &+ \alpha[y(L_{PBU} + \tau(k-2)) + \dots + y(L_{PBU} + \tau) + yL_{PBU}] \theta(k-2) \\
 &+ [(x-1)PC_R + PC_{LMA}] + (k-1)[(y-1)PC_R + PC_{LMA}] \\
 &= \alpha[y((k-1)L_{PBU} + \tau(k-1)(k-2)/2)\theta(k-2) + x(L_{PBU} + \tau(k-1))] \\
 &+ [(x-1) + (k-1)(y-1)]PC_R + k \cdot PC_{LMA},
 \end{aligned} \tag{10}$$

where x is $d_{MAG-LMA}$ and y is $d_{LMA-LMA}$, and the function of $\theta(\bullet)$ is defined as follows:

$$\theta(t) = \begin{cases} 1, & \text{if } t \geq 0, \\ 0, & \text{otherwise.} \end{cases} \tag{11}$$

$$\begin{aligned}
 C_{PBU}(k)|_{\text{wireless}} &= [\beta[L_{PBU} + (L_{PBU} + \tau) + \dots + (L_{PBU} + \tau(k-3)) + (L_{PBU} + \tau(k-2))] \\
 &+ (k-2)PC_{MR} + PC_{MAG}] \theta(k-2) \\
 &= [\beta[(k-1)L_{PBU} + \tau(k-1)(k-2)/2] + (k-2)PC_{MR} + PC_{MAG}] \theta(k-2).
 \end{aligned} \tag{12}$$

$$\begin{aligned}
 C_{PBA}(k)|_{\text{wireline}} &= \alpha[x(L_{PBA} + \tau(k-1)) + y((k-1)L_{PBA} + \tau(k-1)(k-2)/2)\theta(k-2)] \\
 &+ [(x-1) + (k-1)(y-1)]PC_R + (k-1)PC_{LMA} + PC_{MAG},
 \end{aligned} \tag{13}$$

$$C_{PBA}(k)|_{\text{wireless}} = \left[\beta \left[(k-1)L_{PBA} + \tau \frac{(k-1)(k-2)}{2} \right] + (k-1)PC_{MR} \right] \theta(k-2),$$

where x is $d_{LMA-MAG}$ and y is $d_{LMA-LMA}$.

$$\begin{aligned}
 C_{PD}|_{\text{wireless}} &= \beta[E(S)L_p + E(S)(L_p + \tau) + \dots + E(S)(L_p + (M-1)\tau)] + (M-1)PC_{MR} + PC_{MAG} \\
 &= \beta E(S)M \left[L_p + \tau \frac{(M-1)}{2} \right] + (M-1)PC_{MR} + PC_{MAG}.
 \end{aligned} \tag{15}$$

$$\begin{aligned}
 C_{PD}|_{\text{wireline}} &= \alpha[xE(S)(L_p + M\tau) + yE(S)(L_p + (M-1)\tau) \dots + yE(S)(L_p + \tau)] \\
 &+ (x-1)PC_R + PC_{LMA} + [(y-1)PC_R + PC_{LMA}](M-1) + zE(S)L_p + (z-1)PC_R \\
 &= \alpha[xE(S)(L_p + M\tau) + yE(S)(M-1)[L_p + \tau M/2]] \\
 &+ (x-1)PC_R + (M-1)(y-1)PC_R + M \cdot PC_{LMA} + zE(S)L_p + (z-1)PC_R,
 \end{aligned} \tag{16}$$

where x is $d_{MAG-LMA}$, y is $d_{LMA-LMA}$, and z is d_{LMA-CN} .

calculated as follows:

$$\begin{aligned}
 C_{BU}(k) &= [E(H_{k,\text{interMAG}}) + E(H_{k,\text{intraMAG}})] \\
 &\times [C_{PBU}(k)|_{\text{wireline}} + C_{PBU}(k)|_{\text{wireless}} \\
 &+ C_{PBA}(k)|_{\text{wireline}} + C_{PBA}(k)|_{\text{wireless}}].
 \end{aligned} \tag{14}$$

delivery cost in a wireless section as Eq. (15). Considering the nested tunnels between LMAs in a wire-line section, the packet delivery cost is calculated as Eq. (16). Thus, the total packet delivery cost can be obtained as follows:

$$C_{PD} = C_{PD}|_{\text{wireline}} + C_{PD}|_{\text{wireless}}. \tag{17}$$

If we combine Eqs. (14) and (2), then we can obtain the total cost of a binding update in N-PMIPv6.

Let $E(S)$ and L_p be the average session length in the packets and the fixed data packet length, respectively. With the nested tunnel in a wireless section, we get the packet

C. Performance Analysis of TFS

As the specific node at level k moves, the number of moving nodes including hidden nodes is $(1 + U_k)$. Therefore, because signaling procedures are separately performed

per node in a wire-line section, the cost of processing a PBU message is calculated in a wire-line section as follows:

$$C_{PBU}(k)|_{\text{wireline}} = [\alpha x L_{PBU} + (x-1)PC_R + PC_{LMA}] \times (1 + U_k) \quad (18)$$

where x is $d_{MAG-LMA}$. In a wireless section, there are two steps in binding updates, as shown in Fig. 5(b). The first step is the handling of the binding update of a top moving node, and the second step is that of the hidden nodes, as shown in Eq. (19). Similarly, the cost of processing a PBA message can be calculated as Eq. (20). $C_{PBA,RA}(k)|_{\text{wireless}}$ includes the cost of processing a modified RA message as in Fig. 5. In the case of the intra-MAG handover, there are no signaling procedures in the TFS scheme. Therefore, the cost of a binding update is calculated as Eq. (21). With Eq. (21) and (2), we obtain the total cost of a binding update in the TFS scheme. As analyzed in the N-PMIPv6, we get the packet delivery cost with $E(S)$ and L_p as Eq. (22).

V. NUMERICAL RESULTS

In this section, we present and compare the performance results of N-PMIPv6 and TFS. For any numerical result in

which specific system parameters are not provided, the following parameters are used.

- $M = 3$: the nested level of a wireless section
- $S_{M-1} = \pi \cdot (10)^2 \approx 314 \text{ m}^2$: the communication area of MR at level $(M-1)$
- $[N_1, N_2, N_3] = [100, 10, 2]$: the number of nodes connected to one MR or MAG at each level
- $[v_1, v_2, v_3] = [20, 5, 2]$: the velocity (m/s) of nodes at each level
- $E(S) = 45$: the average length of a session in the packets
- $L_p = 300$: the average packet length in bytes

With a fixed session arrival rate λ_s of 0.2, three results are shown in Table 1. In case 1, the weighting factor of level 1 is 1.0 and the other weighting factors are all zero. On the other hand, in case 2, the weighting factor of level 3 is 1.0. From the viewpoint of the signaling cost, case 2 can show the advantages of the TFS scheme, but case 1 corresponds to the worst case of the TFS scheme. There are two key factors affecting the signaling performance. The first factor is the number of hidden nodes. In N-PMIPv6, the signaling cost is not dependent on the number of hidden nodes, but because the TFS scheme requires the binding updates of hidden nodes, the number of hidden nodes has a negative influence on the signaling performance in the TFS scheme. The second key factor affecting the signal performance is the

$$C_{PBU}(k)|_{\text{wireless}} = [\beta(k-1)L_{PBU} + (k-2)PC_{MR} + PC_{MAG}]\theta(k-2) + [\beta(L_{PBU} + \phi U_k)k + (k-1)PC_{MR} + PC_{MAG}]\theta(U_k - 1). \quad (19)$$

$$C_{PBA}(k)|_{\text{wireline}} = [\alpha x L_{PBA} + (x-1)PC_R + PC_{LMA}](1 + U_k), \\ C_{PBA,RA}(k)|_{\text{wireless}} = [\beta L_{PBA} + PC_{MR}](k-1) + [\beta L_{PBA} + PC_{MR}]k U_k + [\beta L_{RA} + PC_{MR}], \quad (20)$$

where x is $d_{MAG-LMA}$.

$$C_{BU}(k) = E(H_{k,\text{interMAG}})[C_{PBU}(k)|_{\text{wireline}} + C_{PBU}(k)|_{\text{wireless}} + C_{PBA}(k)|_{\text{wireline}} + C_{PBA,RA}(k)|_{\text{wireless}}] + E(H_{k,\text{intraMAG}})[C_{PBU}(k)|_{\text{wireless}} + C_{PBA,RA}(k)|_{\text{wireless}}]. \quad (21)$$

$$C_{PD}|_{\text{wireless}} = \beta M \cdot E(S)L_p + (M-1)PC_{MR} + PC_{MAG}, \\ C_{PD}|_{\text{wireline}} = \alpha x \cdot E(S)(L_p + \tau) + (x-1)PC_{MR} + PC_{LMA} + E(S)L_p z + (z-1)PC_R, \\ C_{PD} = C_{PD}|_{\text{wireless}} + C_{PD}|_{\text{wireline}}, \quad (22)$$

where x is $d_{MAG-LMA}$ and z is d_{LMA-CN} .

intra-MAG handover that is the positive factor for the TFS scheme, because the intra-MAG handover does not initiate signaling procedures between the MAG and the LMA. In case 1, a movement of a MN at level 1 causes the simultaneous handover of many hidden nodes at levels 2 and 3. Because N_2 is 10 and N_3 is 2, the total number of hidden nodes is 30 from the viewpoint of a MN at level 1. Therefore, a handover event yields thirty times the binding updates for the hidden nodes and the TFS scheme denotes a larger cost of a binding update than that of N-PMIPv6 in case 1. By contrast, the TFS scheme outperforms N-PMIPv6 in case 2. Handover events of case 2 are mainly the intra-MAG handovers where there are no signaling messages between the MAG and the LMA in the TFS scheme. The reduction of signaling messages results in the lower cost of a binding update in case 2. Depending on several factors (i.e., the moving velocity, the number of MNs at each level, the nested level, and so on), both the N-PMIPv6 and the TFS scheme represent the pros and cons. In the other numerical results, we apply a weighting factor of case 3. Although the signaling cost of TFS is higher than that of N-PMIPv6 in case 3, the remarkable performance of the TFS scheme will be shown on account of the low packet delivery cost.

Table 1. Cost of a binding update according to the weighting factor

Three scenarios	Cost of binding update (C_{BU})	
	N-PMIPv6	TFS
Case 1 ($\omega = [1.0, 0.0, 0.0]$)	661	22291
Case 2 ($\omega = [0.0, 0.0, 1.0]$)	6680	464
Case 3 ($\omega = [0.3, 0.3, 0.4]$)	3853	7235

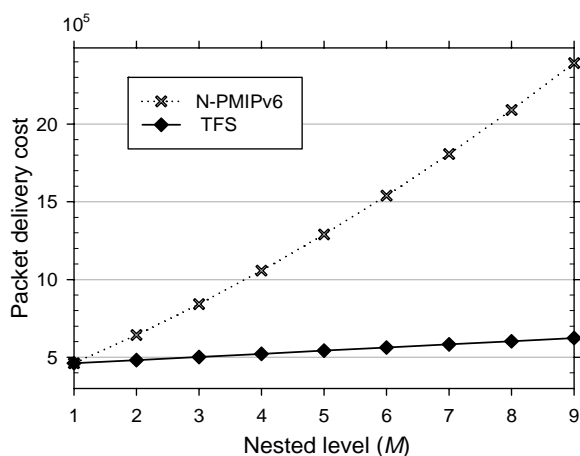


Fig. 7. Packet delivery cost according to the nested level. TFS: tunnel-free scheme.

Fig. 7 shows the difference in the packet delivery cost as a function of various nested levels. As the nested level becomes larger in N-PMIPv6, the packet length becomes larger with nested tunnels and should travel around many LMAs. On the other hand, it is shown in Fig. 7 that the TFS scheme seems insensitive to a change in the nested level. Due to both the route optimization of the wire-line section and the tunnel-free mechanism of the wireless section, the packet delivery cost is much lower than that of N-PMIPv6. However, since the packet delivery cost dominates the signaling performance, our TFS scheme ultimately outperforms N-PMIPv6.

The relationship between the packet delivery cost and the packet length is shown in Fig. 8. As the packet length increases, the packet delivery cost of N-PMIPv6 increases rapidly. The main reason for this large increase is the non-optimal routing path of N-PMIPv6. In the case that the nested level is 1, because there is no tunnel in a wireless section and one tunnel between the MAG and the LMA, the packet delivery cost of the TFS scheme is the same as that of N-PMIPv6. When the nested level is larger than 1, nested tunnels are heavily overlapped in N-PMIPv6 and thus the performance difference becomes conspicuous due to the non-optimal routing path. The performance difference of the packet delivery cost is hundreds or thousands of times larger than that of the signaling cost. That is, although the signaling cost of the TFS scheme is slightly higher than that of N-PMIPv6, the TFS scheme outperforms N-PMIPv6 from the point of view of the total protocol cost. When the average length of the session is larger, the performance difference between N-PMIPv6 and TFS becomes greater. Moreover, as shown in Figs. 7 and 8, the performance variations are relatively small in the TFS scheme.

A greater weight is generally assigned to a one-hop distance in a wireless section than in a wire-line section. This is because the wireless resource is more precious and expensive than the wire-line resource. It needs more time and more cost to send the same amount of data packets in the wireless section than in the wire-line section. When a packet travels along the same hop distance in both a wire-line and a wireless section, the protocol cost is larger in the wireless section than it is in the wire-line section. In the performance analysis, we define the notation β as a transmission unit cost in a wireless link. In Fig. 9, we compare the packet delivery cost with varying β . Because N-PMIPv6 has more overhead due to nested tunnels in a wireless link, it needs to send a larger packet in the wireless link. Thus, as parameter β is increased, the performance difference between TFS and N-PMIPv6 is enlarged.

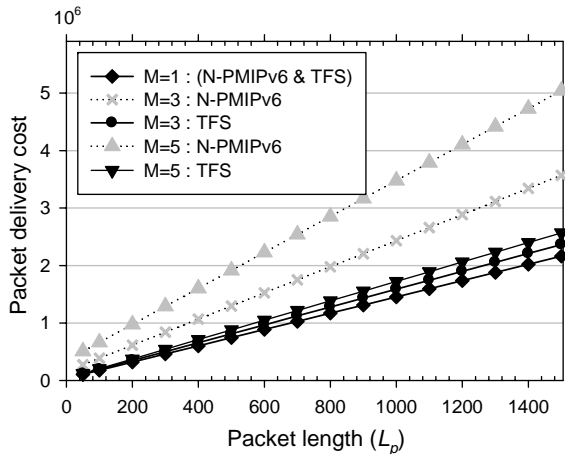


Fig. 8. Packet delivery cost according to the packet length. TFS: tunnel-free scheme.

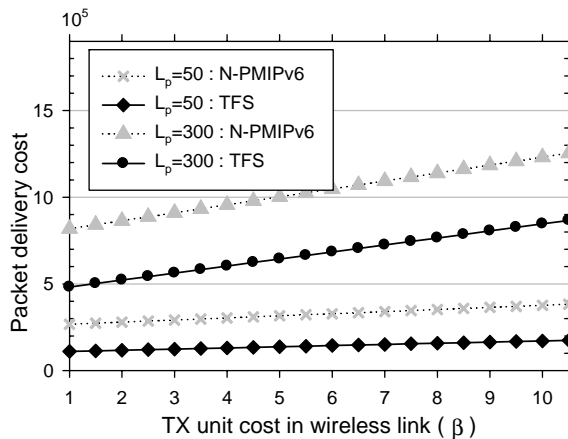


Fig. 9. Packet delivery cost according to the parameter β . TFS: tunnel-free scheme.

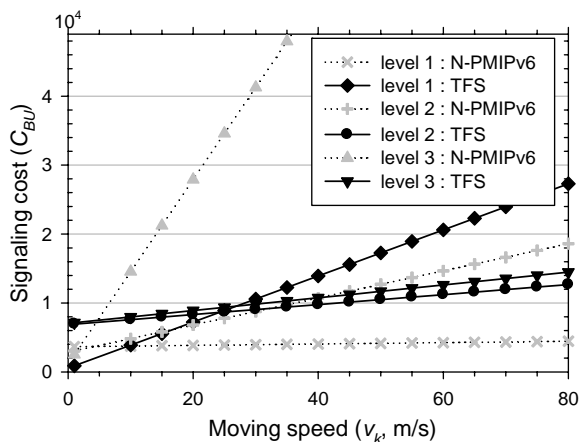


Fig. 10. Signaling cost according to the moving speed. TFS: tunnel-free scheme.

When the nested level is 3, the velocity of each level's node, $[v_1, v_2, v_3]$, is fixed by $[20, 5, 2]$ (m/s). Fig. 10 shows that the signaling cost tends to increase as the moving speed at each level increases. Because the signaling costs are obtained from varying the velocity of three levels, Fig. 10 demonstrates the three different results for N-PMIPv6 and TFS. Only one velocity among the three default values ($[v_1, v_2, v_3] = [20, 5, 2]$) is considered to vary, while the other velocities are fixed in Fig. 10. Let us concentrate on the three results for N-PMIPv6. As the level of the moving nodes becomes higher, the signaling cost in N-PMIPv6 becomes higher, too. This is because the cell size of the higher level is smaller, resulting in many handover events. The signaling cost of the TFS scheme, however, is not always proportional to the level of moving nodes. In order to understand the performance results of the TFS scheme, we should consider two factors: the number of hidden nodes and the effect of the intra-MAG handover. A higher level of a moving node means the number of hidden nodes is smaller, but the number of total handover nodes is larger. The reduction of hidden nodes reduces the signaling cost, such as the cost of a binding update. The increment of handover events results in the higher signaling cost. However, as the level of a moving node is higher, the portion of the intra-MAG handover is larger and it causes a lower signaling cost. Thus, in the TFS scheme, there are both positive and negative factors for signaling costs. Because the intra-MAG handover in the TFS scheme does not generate the signaling procedure between the MAG and the LMA, the portion of the intra-MAG handover plays an important role in the TFS scheme. Fig. 10 also demonstrates that although the signaling cost of the TFS scheme may sometimes be larger than that of N-PMIPv6, TFS is less sensitive to each level's moving speed than N-PMIPv6.

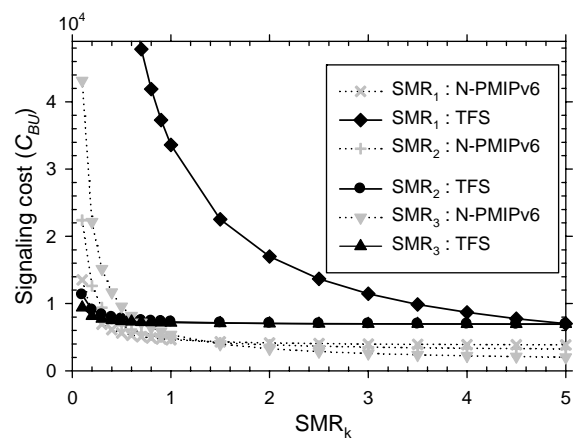


Fig. 11. Signaling cost according to session-to-mobility ratio (SMR). TFS: tunnel-free scheme.

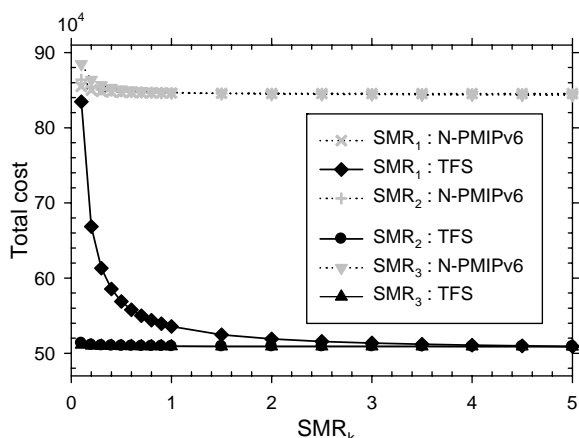


Fig. 12. Total cost according to session-to-mobility ratio (SMR). TFS: tunnel-free scheme.

In Fig. 11, the signaling performance is described according to the variation of each level's SMR. The default values at each level for the SMR are $SMR_1 = 5.0$, $SMR_2 = 2.0$, and $SMR_3 = 1.6$. The performance results of level 1 are obtained under the assumption that the other parameters are fixed as ($SMR_2 = 2.0$, $SMR_3 = 1.6$). Commonly, as the SMR is larger, the mobility is smaller and the signaling cost is reduced. Due to the local binding update of the intra-MAG handover, the signaling cost of the TFS scheme may be lower than that of N-PMIPv6 in some cases, but in most cases TFS has no more advantages over N-PMIPv6 from the perspective of the binding update. However, the packet delivery cost is hundreds of thousands, while the signaling cost is tens of thousands. That is, as described before, the signaling cost is a minor portion of the total protocol cost. Because the packet delivery cost of the TFS scheme is significantly lower than that of N-PMIPv6, our proposed TFS scheme outperforms N-PMIPv6, as shown in Fig. 12. Even though the proposed TFS scheme has a weakness with regard to the signaling cost, it represents superior performance with respect to the total cost.

VI. CONCLUSION

In this paper, we propose the TFS that removes nested tunnels in a wireless section and optimizes the routing path in a wire-line section. Instead of nested tunnels in a wireless section, the TFS scheme uses a host-based routing table and optimizes the routing path between the MAG and the LMA. By removing nested tunnels, the wireless resource utilization is improved and packet fragmentation may be avoided. With routing path optimization, the hop distance between the MAG and the LMA is reduced and

mitigates the load of the LMA. As described in our numerical results, the signaling cost of the TFS scheme may be higher than that of N-PMIPv6 in some cases. However, in view of the packet delivery cost, the TFS scheme outperforms N-PMIPv6. Additionally, as the nested level is larger, the TFS scheme provides remarkably better performance than N-PMIPv6. For further research, we are developing a modification of the TFS scheme as a routing optimization method.

ACKNOWLEDGMENTS

This research was financially supported by the 2012 National Research Foundation of Korea (NRF) research grant (2012-R1A1A2041831).

REFERENCES

- [1] S. Deering and R. Hinden, "Internet protocol, version 6 (IPv6) specification," the Internet Engineering Task Force, Fremont: CA, *RFC 2460*, 1998.
- [2] D. Johnson, C. Perkins, and J. Arkko, "Mobility support in IPv6," the Internet Engineering Task Force, Fremont: CA, *RFC 3775*, 2004.
- [3] S. Gundavelli, K. Leung, V. Devarapalli, K. Chowdhury, and B. Patil, "Proxy mobile IPv6," the Internet Engineering Task Force, Fremont: CA, *RFC 5213*, 2008.
- [4] V. Devarapalli, R. Wakokawa, A. Petrescu, and P. Thubert, "Network mobility (NEMO) basic support protocol," the Internet Engineering Task Force, Fremont: CA, *RFC 3963*, 2005.
- [5] I. Soto, C. J. Bernardos, M. Calderon, A. Banchs, and A. Azcorra, "NEMO-enabled localized mobility support for internet access in automotive scenarios," *IEEE Communications Magazine*, vol. 47, no. 5, pp. 152-159, 2009.
- [6] Z. Yan, H. Zhou, and I. You, "N-NEMO: a comprehensive network mobility solution in proxy mobile IPv6 network," *Journal of Wireless Mobile Networks, Ubiquitous Computing, and Dependable Applications*, vol. 1, no. 2-3, pp. 52-70, 2010.
- [7] M. S. Woo, H. B. Lee, Y. H. Han, and S. G. Min, "A tunnel compress scheme for multi-tunneling in PMIPv6-based nested NEMO," *International Journal of Wireless & Mobile Networks*, vol. 2, no. 4, pp. 60-69, 2010.
- [8] A. Z. M. Shahriar, M. Atiquzzaman, and W. Ivancic, "Route optimization in network mobility: solutions, classification, comparison, and future research directions," *IEEE Communications Surveys & Tutorials*, vol. 12, no. 1, pp. 24-38, 2010.
- [9] J. H. Lee and T. M. Chung, "How much do we gain by introducing route optimization in proxy mobile IPv6 networks?," *Annals of Telecommunications*, vol. 65, no. 5-6, pp. 233-246, 2010.
- [10] F. Abinader, S. Gundavelli, K. Leung, S. Krishnan, and D. Premec, "Bulk re-registration for proxy mobile IPv6," the Internet Eng-

ineering Task Force, Fremont: CA, 2011.

- [11] C. Makaya and S. Pierre, "An analysis framework for performance evaluation of IPv6-based mobility management protocols," *IEEE Transactions on Wireless Communications*, vol. 7, no. 3, pp. 972-983, 2008.

- [12] F. V. Baumann and I. G. Niemegeers, "An evaluation of location management procedures," in *Proceedings of the 3rd Annual International Conference on Universal Personal Communications*, San Diego: CA, pp. 359-364, 1994.



Sunghong Wie

received the B.S., M.S. and Ph.D. degrees in Electrical Engineering from KAIST, South Korea, in 1995, 1997, and 2001, respectively. From 2001 to 2008, he was with Samsung Electronics as a senior engineer. Currently, he is with Division of Information Technology at The Cyber University of Korea. His recent research interests include mobility management and future internet.



Jaeshin Jang

received the B.S. degree in Electrical Engineering from Dong-A University, Korea, in 1990, and the M.S. and Ph.D. degrees in Electrical Engineering from KAIST, Korea, in 1992 and 1998, respectively. From July 1997 to February 2002, he worked for Samsung Electronics Company. From August 2008 to July 2009, he was a visiting scholar at Iowa State University. Since March 2002, he has worked for Inje University, Korea. His major interests are wireless QoS, MAC, routing, and cooperative communications at wireless communications networks, including mobile WiMAX, ad-hoc networks, and mesh networks.